

Supporting Information for

Original article

Histone deacetylase inhibitors inhibit cervical cancer growth through Parkin acetylation-mediated mitophagy

Xin Sun^a, Yuhan Shu^d, Guiqin Ye^c, Caixia Wu^b, Mengting Xu^d, Ruilan Gao^e, Dongsheng Huang^{c,*}, Jianbin Zhang^{b,*}

^aDepartment of Oncology, Zhejiang Provincial People's Hospital, Affiliated People's Hospital, Hangzhou Medical College, Hangzhou 310014, China

^bClinical Research Institute, Zhejiang Provincial People's Hospital, Affiliated People's Hospital, Hangzhou Medical College, Hangzhou 310014, China

^cKey Laboratory of Tumor Molecular Diagnosis and Individualized Medicine of Zhejiang Province, Hangzhou Medical College, Hangzhou 310014, China

^dCollege of Biomedical Engineering & Instrument Science, Zhejiang University, Hangzhou 310028, China

^eDepartment of Hematology, the First Affiliated Hospital of Zhejiang Chinese Medical University, Hangzhou 310006, China

Received 8 February 2021; received in revised form 30 May 2021; accepted 16 June 2021

*Corresponding authors.

E-mail addresses: zhangjianbin@hmc.edu.cn (Zhang Jianbin), dshuang@zju.edu.cn (Huang Dongsheng).

Running title: Parkin acetylation enhances mitophagy

1. Supporting tables

Table S1 The specific targets of Parkin under SAHA treatment was identified and listed.

Table S2 GO analysis of the Parkin targets. The Parkin-targeted mitochondrial proteins and their molecular functions were listed.

Molecular function	Protein No.	Protein name
Oxidoreductase	6	ALDH18A1, ALDH5A1, ALDH1B1, ALDH2, ALDH5, ALDH3A2
Isocitrate dehydrogenase	4	IDH3G, IDH2, IDH3B, IDH3A
Phosphatase	5	PDP1, TIMM50, PPP3CA, PPP1CC, PTEN
C-Acetyltransferase	7	ACAA2, GCAT, ACSL3, ACAT1, SCP2, HADHA, HADHB
Voltage-gated anion channel	4	CLIC4, VDAC2, VDAC3, VDAC1
Peroxidase	4	PRDX4, PRDX3, CAT, PRDX1
Transmembrane transporter	9	ATP6V1A, UQCRC1, ATP6V1E1, ATP5F1, ATP5O, COX5A, MON2, SLC25A4, SLC25A5
Hexokinase	2	HK2, HK1
Succinate dehydrogenase	2	SDHA, SDHB
Creatine kinase	2	CKMT1A, CKB
Succinyltransferase	2	DLST, ALAS1

Table S3 The detailed MS spectra of Parkin acetylation sites are shown.

2. Supporting figures

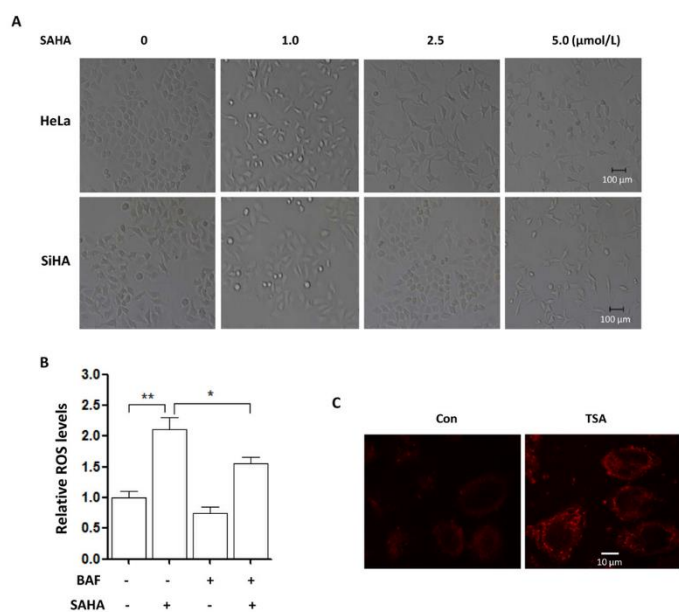


Figure S1 Autophagy inhibition attenuates ROS production under SAHA treatment. (A) Morphology of HeLa and SiHA cells was captured using a phase contrast microscopy. Scale bar=100 μm . (B) HeLa cells were transfected with the mKeima-Red-Mito-7 plasmid, followed by treatment with TSA (0.5 $\mu\text{mol/L}$, 1 h). The fluorescence was detected by confocal microscope. Scale bar=10 μm . (C) SiHA cells were given SAHA treatment with or without bafilomycin A1 (10 nmol/L). Mitochondrial ROS was detected by MitoTracker™ Red CMXRos staining and quantified by flow cytometry. * $P < 0.05$, ** $P < 0.01$.

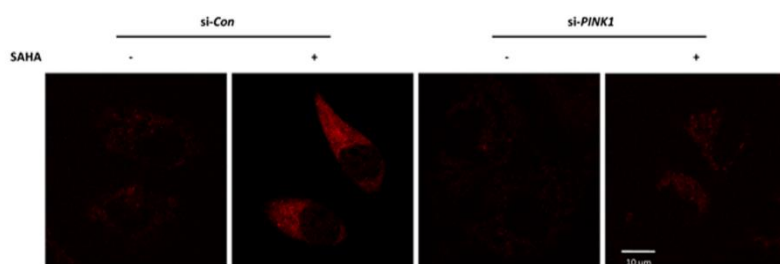


Figure S2 SAHA-induced mitophagy depends on the PINK1 pathway. SiHA cells expressing mKeima-Red-Mito-7 were first transfected with the *PINK1*-specific siRNA and then cells were treated with SAHA (5 $\mu\text{mol/L}$, 12 h). The fluorescence was detected by Confocal Microscope. Scale bar=10 μm .

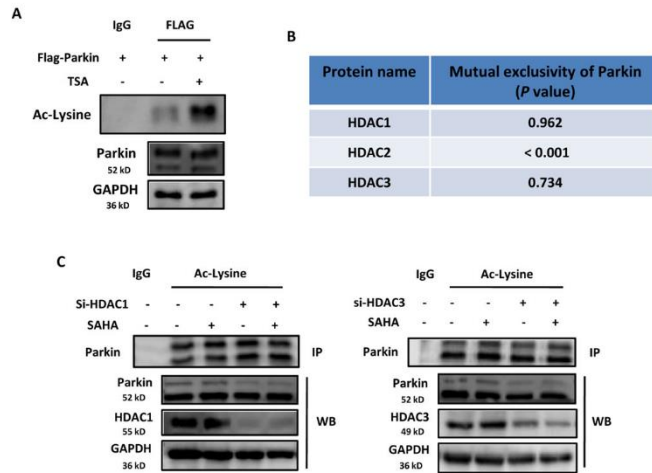


Figure S3 HDAC inhibition leads to Parkin acetylation. (A) HEK293 cells were transiently transfected with Flag-Parkin and then treated with 1 μ mol/L TSA for 12 h. Cells were lysed and subjected to FLAG immunoprecipitation followed by immunoblotting for acetyl-lysine. (B) Analysis of mutual exclusivity of Parkin with HDAC1/2/3 using cBioPortal for Cancer Genomics. (C) HEK293 cells were transiently transfected with Flag-Parkin, together with specific siRNA for *HDAC1* or *HDAC3*. After SAHA treatment, cell lysates were prepared and immunoprecipitated with acetyl-lysine and immunoblotted for Parkin.

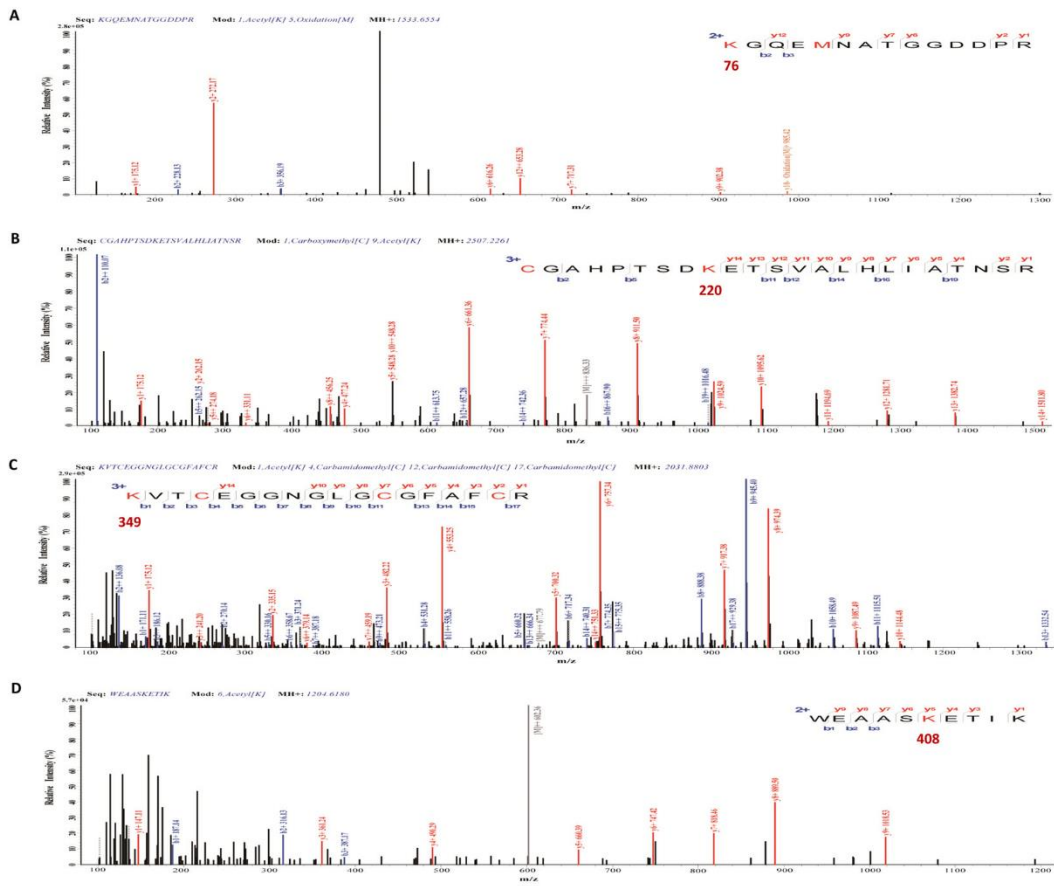


Figure S4 The LC-MS spectra of the peptide contains the acetylated K76, K220, K349, and K408. Fragment ions containing acetylated lysine are denoted by red color.

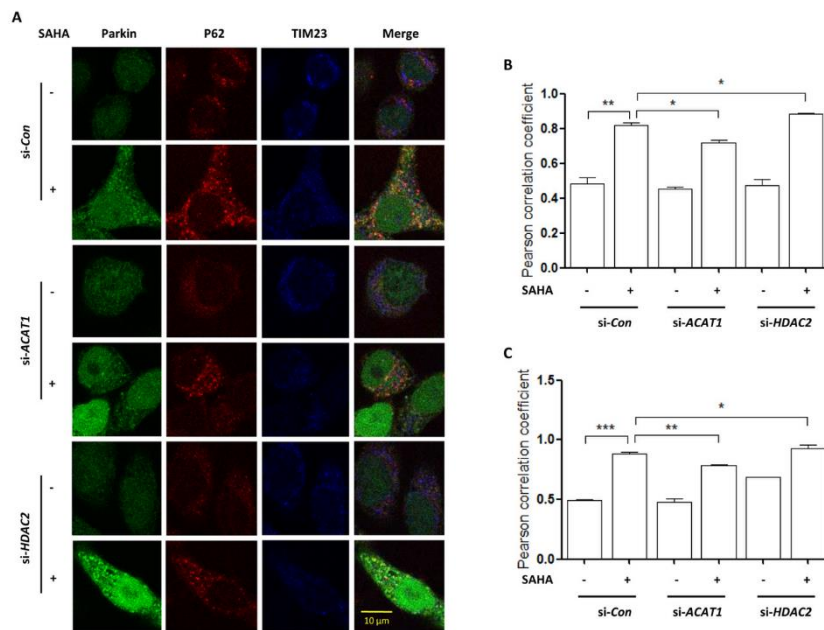


Figure S5 ACAT1 and HDAC2 control Parkin translocation to mitochondria under SAHA treatment. (A) and (B) HeLa cells with YFP-Parkin overexpression were

transfected with specific siRNA for *ACAT1* or *HDAC2*, respectively, and treated with SAHA (5 $\mu\text{mol/L}$, 12 h). Confocal imaging of P62 (red) and TIM23 (blue) was conducted. Scale bar=10 μm . ImageJ was used to analyze their colocalization and statistics was performed. * $P<0.05$, ** $P<0.01$, *** $P<0.001$. (C) ImageJ was used to analyze the colocalization of GFP-LC3, LAMP1 and TIM23, and statistics was performed.

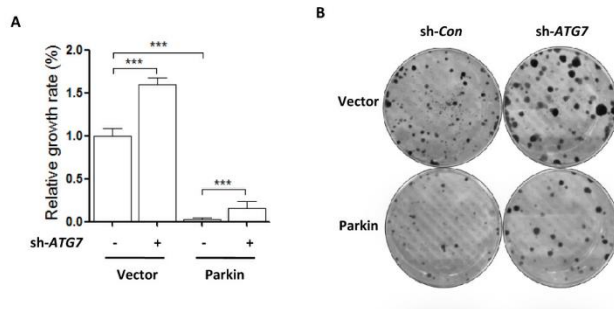


Figure S6 Knockdown of *ATG7* attenuates the inhibitory effect of Parkin on cell growth. HeLa cells with or without Parkin expression were infected with lentivirus expressing nonspecific shRNA or specific shRNA for *ATG7*. (A) Cells were seeded into 96-well plate and cell proliferation was measured by adding CCK-8 solution. The absorbance was measured at 450 nm using microplate spectrophotometer and statistically analyzed. *** $P<0.001$. (B) Cells were seeded into 6-well plate and colony formation assay was performed to determine cell proliferation. After crystal violet staining, the formed colonies were photographed.

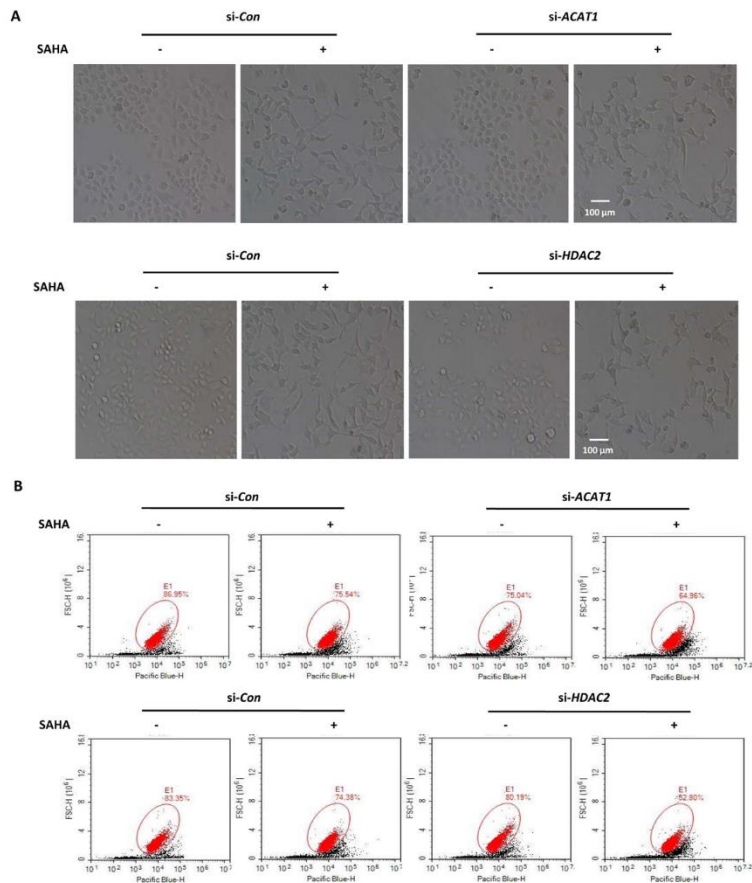


Figure S7 ACAT1 and HDAC2 regulate cell death by SAHA treatment. SiHA cells were first transfected with specific siRNA for *ACAT1* or *HDAC2*, and then treated with SAHA (5 $\mu\text{mol/L}$, 24 h). (A) Cell morphology was photographed using a phase-contrast microscope. Scale bar=100 μm . (B) Cells were stained using the Annexin V, Pacific Blue™ conjugate and cell fluorescence was shown in flow cytometry graph.

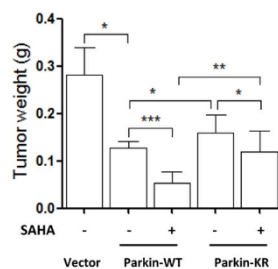


Figure S8 Parkin mutation attenuates the anticancer activity of SAHA treatment. The average tumor weight for each group was calculated and statistically analyzed.

* $P < 0.05$, ** $P < 0.01$, *** $P < 0.001$.